

REVERSED FLOW CALCULATIONS OF HIGH PRANDTL NUMBER THERMAL BOUNDARY LAYER SEPARATION¹

J. T. Ratnanather and P. G. Daniels

Department of Mathematics

City University

London, England, EC1V 0HB

ABSTRACT

A numerical and analytical study of the free convection thermal boundary layer or wall jet at finite Prandtl number is performed to understand the mechanisms of the separation of a high Prandtl number thermal boundary layer flows. The model is that adopted by Smith & Duck (1977) in which the upstream influence delineates the flow into a ‘double-deck’ structure with the lower deck having thickness $O(R^{-3/14})$, R being the Rayleigh number. The velocities and pressure in the lower deck are obtained thus determining the temperature distribution in the reversed flow zone. The asymptotic structure of the flow downstream of separation for the temperature is analysed indicating a functional dependence on the streamfunction in the slowly recirculating inviscid core.

1 INTRODUCTION

There are many examples of fluid flows in technology and engineering where imposed boundary conditions or geometries results in flow separation. In applications where thermal effects are significant, such as cooling or insulating systems, such separations can have important consequences for the heat transfer properties of the system. In the present paper we consider the manner in which a thermal jet flow, such as that driven by buoyancy along a heated vertical wall, can separate resulting in a drastic reduction in heat transfer through the wall. Such separations may be relevant, for example, where the jet encounters a corner, obstruction or sudden change in thermal boundary conditions.

One important aspect of such flows is the rôle of the Prandtl number, σ . An eventual aim of the present work is to investigate the flow development at high Prandtl numbers where inertial effects are suppressed at the expense of buoyancy, leading to the possibility of the thermal field playing a significant rôle in the local separation process. Here results are presented for the separation zone at finite Prandtl numbers, where locally the flow is controlled by viscosity and inertia, independent of thermal effects. Nevertheless the resulting

¹Presented at 4th International Symposium on Transport Phenomena in Heat and Mass Transfer, University of New South Wales, Sydney, Australia. July 14-18, 1991.

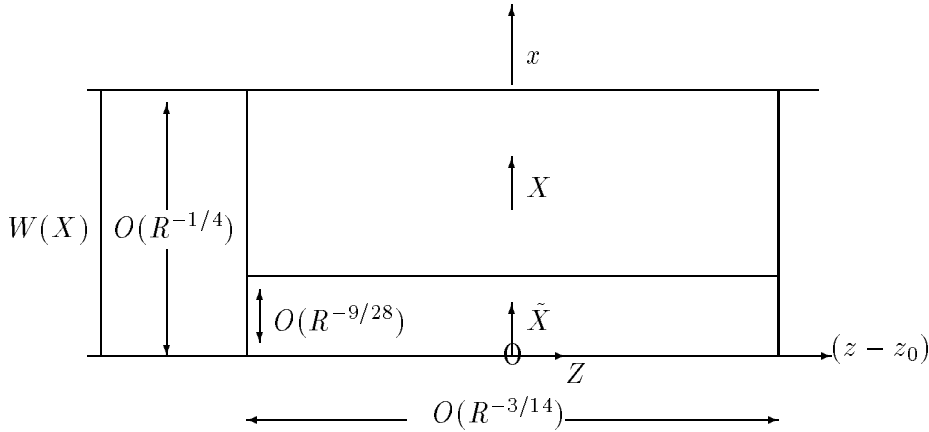


Figure 1: The double deck structure: the sketch has been rotated 90° degrees.

temperature field is of some interest and its calculation is a natural first step in the analysis of high Prandtl number separating flows.

2 PROBLEM FORMULATION

The solution of a vertical thermal boundary layer flow at high Rayleigh numbers, R , was obtained by Gill (1966); it may be represented by the following elementary functions:

$$\psi = R^{1/4}\Psi(X), \quad u = 0, \quad w = R^{1/2}W(X), \quad T = z + \Theta(X),$$

where $x = R^{-1/4}X, z$ are the horizontal and vertical coordinates respectively; u, w are the corresponding velocity components.

At finite Prandtl numbers, the separation of a boundary layer from the wall can occur as a local interaction of the type described by Smith and Duck (1977). In this case, a double deck occurs on a vertical streamwise scale of $Z = O(1)$ where $z = R^{-3/14}Z$ with a main deck where $X = O(1)$ and a lower deck where $\tilde{X} = O(1)$ with $x = R^{-9/28}\tilde{X}$. Fig. 1 demonstrates the double deck structure of the flow undergoing free interaction.

If, in the lower deck,

$$\begin{aligned} u &= R^{9/28}\tilde{U}(\tilde{X}, Z), & w &= R^{3/7}\tilde{W}(\tilde{X}, Z), \\ p &= R^{6/7}\tilde{P}(Z), & T &= R^{-1/14}\tilde{T}(\tilde{X}, Z), \end{aligned}$$

then the following equations describe the steady flow:

$$\frac{1}{\sigma} \left(\tilde{U} \frac{\partial \tilde{W}}{\partial \tilde{X}} + \tilde{W} \frac{\partial \tilde{W}}{\partial Z} \right) + \frac{d\tilde{P}}{dZ} - \frac{\partial^2 \tilde{W}}{\partial \tilde{X}^2} = 0, \quad (1)$$

$$\frac{\partial \tilde{U}}{\partial \tilde{X}} + \frac{\partial \tilde{W}}{\partial Z} = 0, \quad (2)$$

$$\tilde{U} \frac{\partial \tilde{T}}{\partial \tilde{X}} + \tilde{W} \frac{\partial \tilde{T}}{\partial Z} - \frac{\partial^2 \tilde{T}}{\partial \tilde{X}^2} = 0, \quad (3)$$

with:

$$\tilde{U} = \tilde{W} = \tilde{T} = 0 \text{ at } \tilde{X} = 0,$$

and

$$\left. \begin{aligned} \tilde{W} &\sim W'(0)(\tilde{X} + A(Z)) \\ \tilde{T} &\sim \Theta'(0)(\tilde{X} + A(Z)) \end{aligned} \right\} \text{ as } \tilde{X} \rightarrow \infty,$$

where the free interaction condition is given by:

$$\frac{d^2 A}{dZ^2} = -\frac{\sigma \tilde{P}(Z)}{\int_0^\infty W^2 dX}. \quad (4)$$

Thus at leading order, the buoyancy term is not present in the momentum equation. The above equations may be normalised as follows:

$$\begin{aligned} \hat{U} &= W'(0)^{-2/5} \gamma^{-3/5} \sigma^{5/7} \tilde{U} \\ \hat{W} &= W'(0)^{-3/5} \gamma^{1/5} \sigma^{2/7} \tilde{W} \\ \hat{X} &= W'(0)^{2/5} \gamma^{2/5} \sigma^{2/7} \tilde{X} \\ \hat{Z} &= W'(0)^{1/5} \gamma^{1/5} \sigma^{-1/7} Z \\ \hat{P} &= W'(0)^{-6/5} \gamma^{3/5} \sigma^{-3/7} \tilde{P} \\ \hat{T} &= W'(0)^{2/5} \Theta'(0)^{-1} \gamma^{2/5} \sigma^{2/7} \tilde{T} \\ \hat{A} &= W'(0)^{2/5} \gamma^{1/5} \sigma^{2/7} A \end{aligned}$$

where $\gamma := 1/\int_0^\infty W^2 dX$. On dropping the hat symbol, the fundamental equations reduce to:

$$U \frac{\partial W}{\partial X} + W \frac{\partial W}{\partial Z} + \frac{dP}{dZ} - \frac{\partial^2 W}{\partial X^2} = 0, \quad (5)$$

$$\frac{\partial U}{\partial X} + \frac{\partial W}{\partial Z} = 0, \quad (6)$$

$$U \frac{\partial T}{\partial X} + W \frac{\partial T}{\partial Z} - \frac{1}{\sigma} \frac{\partial^2 T}{\partial X^2} = 0, \quad (7)$$

with

$$U = W = T = 0 \text{ at } X = 0,$$

and

$$\left. \begin{aligned} W &\sim X + A(Z) \\ T &\sim X + A(Z) \end{aligned} \right\} \text{ as } X \rightarrow \infty,$$

where

$$\frac{d^2 A}{dZ^2} = -P(Z). \quad (8)$$

A consequence of the normalisation is that the temperature T is decoupled from the velocity field whence it suffices to determine the velocity and the pressure first and then determine

the temperature for a given Prandtl number, σ . For the solution of the velocities and pressure, we follow Smith and Duck (1977). The equations may be expressed in terms of ψ, W and τ where ψ is the streamfunction ($W = \partial\psi/\partial X, U = -\partial\psi/\partial Z$) and $\tau = \partial W/\partial X$ is the stress. The Keller Box scheme (Keller, 1974) is applied to the resulting system of first order partial differential equations with the central differencing centred at the node $(Z_{i-1/2}, X_{j-1/2})$. The nonlinear discrete equations are solved by a Newton-Raphson scheme. Boundary conditions at $X = 0$ and $X = X_\infty$ are prescribed where X_∞ is a suitably chosen large number. Forward marching in the Z direction is adopted with the proviso that at each Z_i station, if $W_{i-1/2, j-1/2} < 0$, as might happen in reversed flows, the discrete form of the streamwise convection term, $W\partial W/\partial Z$ is neglected. Known as the FLARE approximation (Flügge-Lotz and Reyhner, 1968; Stewartson and Williams, 1969) the effect is to avoid any numerical instabilities due to the march in the direction opposite to the backflow at the expense of accuracy. FLARE may be used as a starting point in an iteration scheme which allows one to integrate from downstream into the reversed flow yielding a more accurate picture of the flow. This leads to the necessary specification of a downstream boundary condition.

But in order to initiate the forward marching, boundary conditions upstream of the interaction zone are required. This may be done numerically by assuming the flow is unchanged i.e. $W = X, U = 0$ at $Z = 0$ with a small pressure disturbance. Analytically we may appeal to the Lighthill (1953) solution; see also Stewartson and Williams (1969) and Smith and Duck (1977). For if, Z is large and negative,

$$W = X + f'(X)e^{\lambda Z}, \quad U = -\lambda f(X)e^{\lambda Z}, \quad P = be^{\lambda Z},$$

then it may be shown that, to leading order in $e^{\lambda Z}$,

$$f'(X) = \frac{\lambda^{1/3}b}{Ai'(0)} \int_0^Y Ai(q) dq, \quad Y = \lambda^{1/3}X \quad \text{with } \lambda = (-3Ai'(0))^{3/7}.$$

where $Ai(x)$ is the Airy function. Thus the wall shear stress is given by:

$$\tau = 1 - 3\lambda^{-5/3}bAi'(0),$$

which means that a rise in the pressure ($b > 0$), which might be expected to occur in a separating boundary layer, corresponds to a decrease in the wall shear stress. This upstream influence may manifest itself in the numerical calculations as a boundary condition:

$$\frac{\partial W}{\partial Z} = \lambda(W - X).$$

It is possible to derive a similar expression for the temperature but the analysis is too complicated to present here. In our case, we have imposed a numerical value for the pressure disturbance, say 10^{-4} which is sufficient to cause separation.

Fig. 2 shows the streamwise behaviour of the pressure, wall shear stress and the displacement function (P, τ, A respectively). The characteristic features of free interacting boundary layers are reproduced (Stewartson and Williams, 1969; Smith and Duck, 1977). Note that the plots have been shifted to coincide with $\tau = 0$ at the origin where separation occurs.

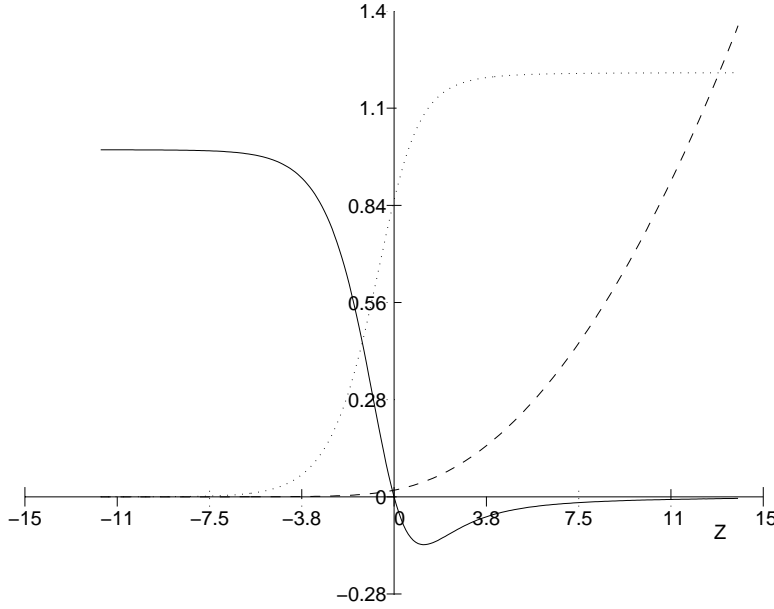


Figure 2: Profiles for P (---), τ (—) and A (...) with upstream conditions at $Z \approx -12.1$.

Note that the pressure approaches a constant value, say P_0 , downstream of separation. This suggests an asymptotic structure for the flow in this region. Assuming that the flow is self preserving, by appealing to the results of Stewartson and Williams (1973) (and also Smith and Duck (1977)), the pressure and displacement function attain the forms:

$$P(Z) = P_0 - \frac{P_1}{2} Z^{-8/3} + O(Z^{-11/3}), \quad A(Z) = -\frac{P_0}{2} Z^2 + O(1).$$

where P_1 is an unknown constant. The velocity field may be composed of three zones: an inner shear layer which is confined to the wall and moves along the wall towards the point of separation, an inviscid recirculating core and an outer shear layer which is the upstream shear layer that has been convected away from the wall. The asymptotic structure is summarised as follows:

- (i) outer shear layer is centred about $X = -A(Z)$ with the streamfunction defined by $\psi = Z^{2/3} G(\xi) + O(1)$ where $\xi = (X + A)/Z^{1/3}$, then the equation of momentum reduces to

$$G''' + \frac{2}{3} G'' G - \frac{1}{3} G'^2 = 0 \quad (9)$$

with $G'(-\infty) = 0$ and $G - \xi^2/2 \rightarrow 0$ as $\xi \rightarrow \infty$ to ensure that the flow matches with the main deck profile and the inviscid core. Numerical solution yields the property $G(-\infty) = -\alpha \approx -1.257$ (cf. Stewartson and Williams (1973)).

- (ii) inviscid core has thickness $O(Z^2)$. Thus, if $\zeta = X/Z^2$ then the streamfunction is $\psi = -aX^{2/3}\zeta$ where a is controlled by the flow in the inner shear layer.

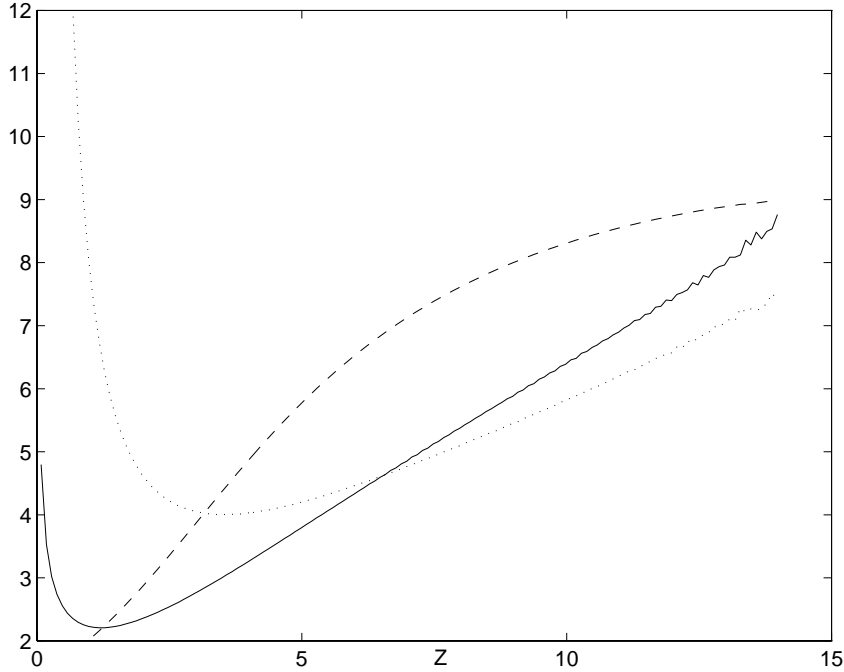


Figure 3: Asymptotic behaviour of $(P_0 - P)^{-3/8}$ (---), $(-\tau_0)^{-2/5}$ (-) and $(-U_{min})^{-3/4}$ (...).

- (iii) inner shear layer is described by $\psi = Z^{-1/6}F(\eta) + O(Z^{-5/6})$ where $\eta = XZ^{-7/6}$.
A Falkner-Skan type equation ensues:

$$F''' - \frac{1}{6}F''F - \frac{4}{3}(F'^2 - P_1) = 0 \quad (10)$$

with the boundary conditions $F(0) = F'(0) = 0$ and $F'(\infty) = -P_1^{1/2}$. Thus matching with the inviscid core gives $a^2 = P_1$. Numerical solution yields the property: $F''(0) = -1.343P_1^{3/4}$ (cf. Smith and Duck (1977)).

Numerical confirmation of this asymptotic structure is evident in fig. 3; we used $P_0 = 1.22$. Finally the flow may be uniquely determined in terms of P_0 via matching of streamfunction in various zones to give

$$P_1 = \frac{4\alpha^2}{P_0^2}.$$

Having determined the asymptotic structure downstream of separation, we intend to adopt the iterative scheme of Williams (1975) in which integrating into a suitably chosen backflow region we can determine the velocities more accurately than FLARE. Known as Downstream Upstream ITerative (DUIT), the algorithm starts with forward marching from the point of separation using FLARE until a suitable value of P_0 is determined along with X_0 which is the limit of the backflow region. With these parameters, the asymptotic profiles may be determined from the above equations. Then with the streamwise convection term $W\partial W/\partial Z$ known, integration into the backflow is permitted and the whole process is repeated until the downstream conditions agree. For the temperature profiles, we expect to adopt a similar strategy but first the asymptotic structure for the temperature has to be determined.

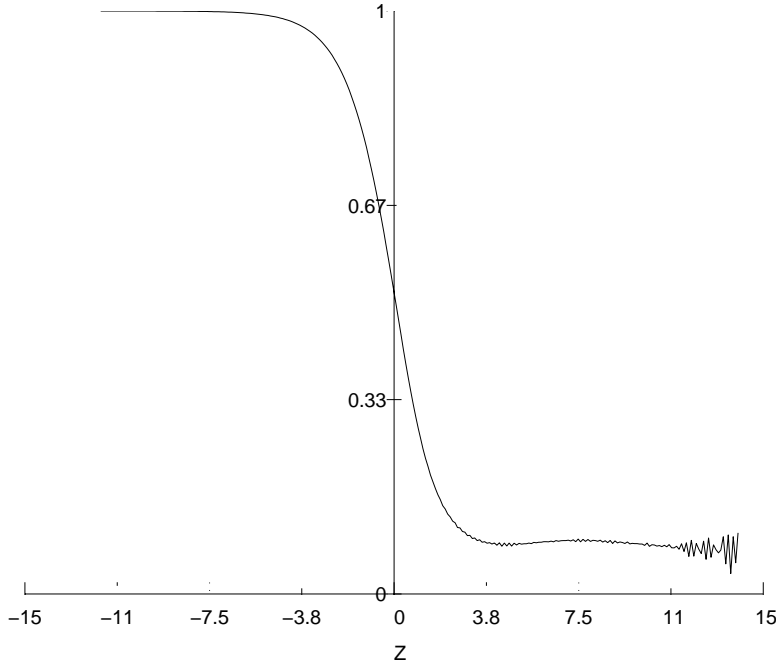


Figure 4: Streamwise development of the wall temperature gradient, $\partial T/\partial X|_{X=0}$, for $\sigma = 1$

3 TEMPERATURE PROFILES

Since the velocity field is already determined, we are left with a linear equation in T for a given Prandtl number σ . As for the velocities, the Keller box scheme is used to set up the discrete equations along with FLARE as a starting point. Fig. 4 shows the temperature gradient at the wall for $\sigma = 1$. It is evident that there is loss of heat transfer in the reversed flow region. However, the wiggles which become prominent downstream of separation give cause for concern. At higher values of σ these wiggles become progressively worse. Whether it is a characteristic feature of the cell Peclet number being greater than 2 (leading to the need for upwinding) or a feature of the FLARE scheme being used, it is prudent, and useful, to consider the asymptotic structure for the temperature profiles downstream of separation. As in the previous section the flow is delineated into three zones summarised as follows:

3.1 Outer shear layer

In the outer shear layer we have $T = Z^{1/3}H(\xi)$ yielding

$$H'' - \frac{\sigma}{3}(G'H - 2GH') = 0, \quad (11)$$

with $H(\infty) = \xi$ to match with the temperature at the upper edge of the lower deck. But for $\xi \rightarrow -\infty$, we have

$$H'' + \frac{2\sigma\alpha}{3}H' = 0,$$

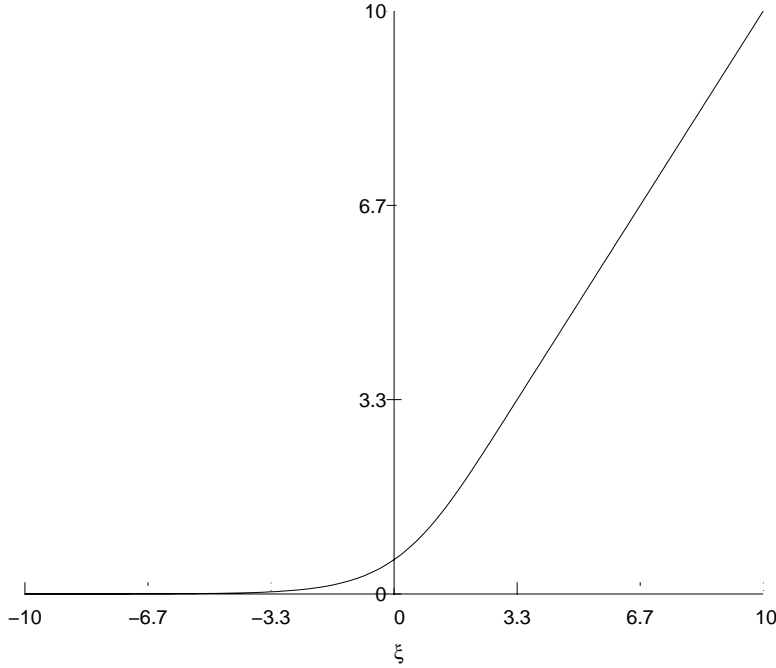


Figure 5: First fundamental solution of outer shear layer temperature equation with $H(-\infty) \sim 0, H(\infty) \sim \xi, \sigma = 1$. Note that $H = G'$.

and since $G(-\infty) = -\alpha$ the general solution at $\xi \sim -\infty$ is

$$H \sim A + B \exp\left(\frac{2\sigma\alpha}{3}\xi\right).$$

That there are two fundamental solutions to eq. 11 may be seen in figs. 5-6 which depict the solutions for

$$H(-\infty) \sim 0 \quad H(\infty) \sim \xi$$

$$\text{or} \quad H(-\infty) \sim 1 \quad H(\infty) \sim 0.$$

Fig. 7 shows that the temperature can attain a minimum in the shear layer before approaching its inviscid core value. Of interest, therefore, is the relationship between the parameters A, B and the inviscid core temperature.

3.2 Inviscid core

The temperature may be expressed as $T = Z^{1/3}S(\zeta)$. Hence the equation for S is:

$$S - 2\zeta S' = 0$$

yielding the general solution $S = K\zeta^{1/2}$. This implies that T may be related to the stream-function by $T = K(-\psi/a)^{1/2}$. K is a constant to be determined that influences the choice of A, B above.

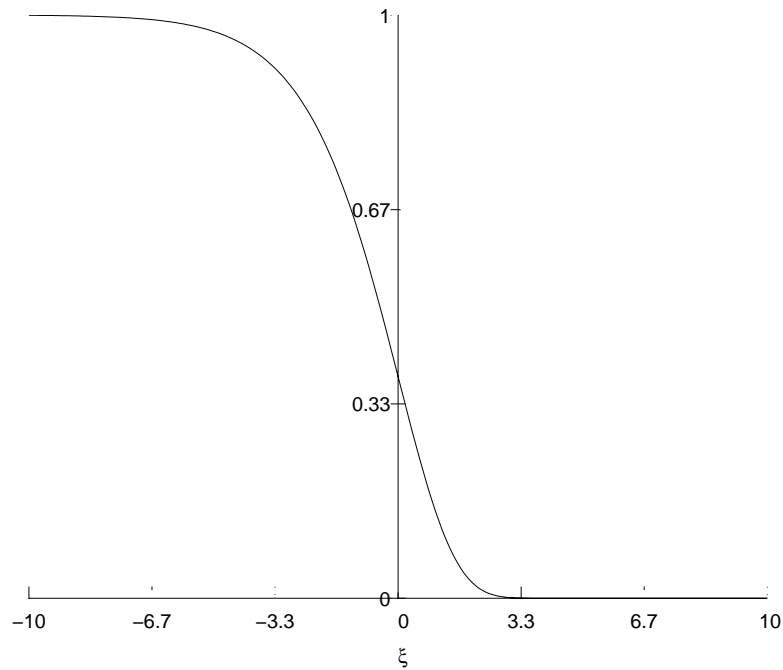


Figure 6: Second fundamental solution of outer shear layer temperature equation with $H(-\infty) \sim 1, H(\infty) \sim 0, \sigma = 1$.

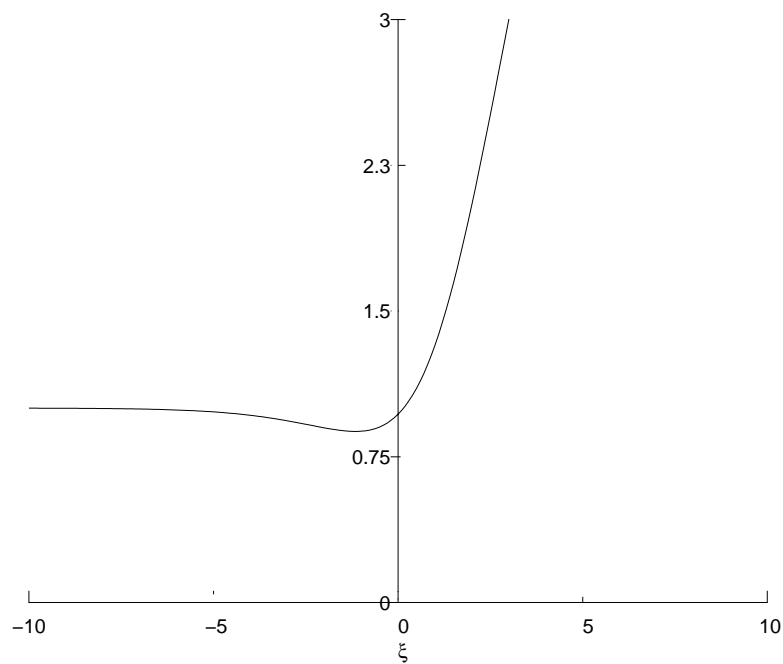


Figure 7: Existence of a minimum in the temperature profile in the outer shear layer with $H(-\infty) = 1, H(\infty) \sim \xi, \sigma = 1$.

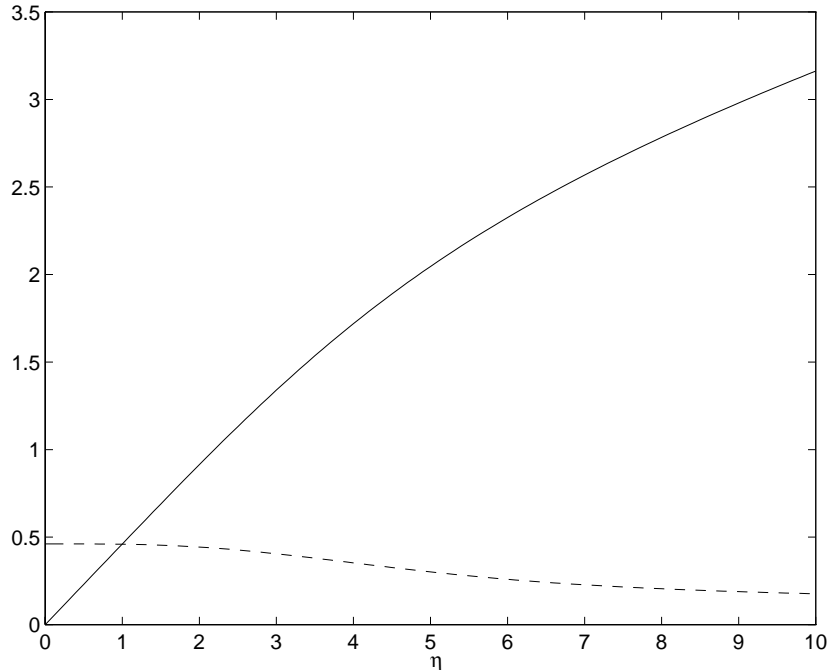


Figure 8: Inner shear layer temperature behaviour, Q (—) and Q' (---), with $Q \sim \eta^{1/2}$, $\eta \rightarrow \infty$, $\sigma = 1$.

3.3 Inner shear layer

Finally, let $T = Z^{-1/12}Q(\eta)$ yielding an equation for Q :

$$Q'' + \frac{\sigma}{12}(F'Q - 2FQ') = 0 \quad (12)$$

with the boundary conditions $Q(0) = 0$ and $Q \sim C\eta^{1/2}$, $\eta \rightarrow \infty$, the latter being a consequence of the matching with the inviscid core temperature. Fig. 8 shows the variation of Q across the inner shear layer. The definition of Q suggests that $(\partial T/\partial X(X=0))^{-4/5}$ should develop linearly with respect to Z downstream of separation but the oscillations in the reversed flow region masks this variation. Hence it is imperative to adopt a DUIT type scheme for the temperature field before any firm conclusions can be made about the high Prandtl number calculations for the temperature field in the reversed flow region.

4 CONCLUSIONS

The preliminary results presented here indicate how separation leads to a sudden reduction of wall heat transfer. As the shear layer departs from the neighbourhood of the wall it carries with it the heat flux contained in the upstream jet flow, leaving a slowly moving region of reverse flow closer to the wall. Here the flow is convectively dominated except in a boundary layer immediately adjacent to the wall and it appears that the temperature field may only be determined uniquely by specification of its precise functional dependence on streamfunction downstream of the separation.

References

- Flügge-Lotz, I. and Reyhner, T. A. (1968). The interaction of a shock wave with a laminar boundary layer. *Int. J. Non-linear Mech.*, *3*, 173–179.
- Gill, A. E. (1966). The boundary layer régime for convection in a rectangular cavity. *J. Fluid Mech.*, *26*, 515–536.
- Keller, H. B. (1974). Accurate difference methods for two-point boundary value problems. *SIAM J. Num. Anal.*, *11*, 305.
- Lighthill, M. J. (1953). On boundary layers and upstream influence II. Supersonic flows without separation. *Proc. Roy. Soc. London*, *A217*, 478–507.
- Smith, F. T. and Duck, P. W. (1977). Separation of jets or thermal boundary layers from a wall. *Q. Jl. Mech. Appl. Math.*, *30*(2), 143–156.
- Stewartson, K. and Williams, P. G. (1969). Self induced separation. *Proc. Roy. Soc. London*, *A312*, 181–206.
- Stewartson, K. and Williams, P. G. (1973). Self induced separation II. *Mathematika*, *20*, 98–108.
- Williams, P. G. (1975). A reverse flow computation in the theory of self-induced separation. *Lecture Notes in Physics*, *35*, 445–451.